Shahtaj, S., Fan, F., Arshad, A., & Stewart, B. (in press). DC needle-plane PD measurements with superimposed harmonics. Paper presented at 2024 IEEE Electrical Insulation Conference, Minneapolis, Minnesota, United States.

DC Needle-Plane PD Measurements with Superimposed Harmonics

Shahtaj Shahtaj
Institute for Energy and Environment
University of Strathclyde
Glasgow, United Kingdom
shahtaj@strath.ac.uk

Fulin Fan
Institute for Energy and Environment
University of Strathclyde
Glasgow, United Kingdom
f.fan@strath.ac.uk

Arshad Arshad
Department of Electrical and Electronic Engineering
Glasgow Caledonian University
Glasgow, United Kingdom
arshadali.giki@gmail.com

Brian G. Stewart
Institute for Energy and Environment
University of Strathclyde
Glasgow, United Kingdom
brian.stewart.100@strath.ac

***Abstract*—High voltage direct current (HVDC) transmission systems play a crucial role in addressing the challenges associated with the delivery of renewable energy by enhancing transmission capacity. However, their reliance on converters makes them susceptible to the issues related to current harmonics and voltage distortions. It is worth noting that, as of now, harmonics are not typically regarded as detrimental in HVDC systems. Nevertheless, there is a growing concern about their potential impacts on the occurrence of partial discharges (PDs) in cable systems that can cause the degradation of cable insulation. To provide insights into PD behavior under DC voltage superimposed harmonics, the paper investigates PD measurements on a needle-plane electrode configuration following the IEC-60270 standard and applying the stresses of PD inception voltage (PDIV) and 1.5 times PDIV under different harmonic components. The comparative analysis and discussion of PD patterns under different superimposed voltage harmonics are presented, considering effective Phase Resolved PD (PRPD) patterns, PD repetition rates, and severity factors.**

Keywords—Harmonics, IEC-60270, Phased Resolved Partial Discharge, repetition rate, severity factor.

I. INTRODUCTION

High voltage direct current (HVDC) cables are widely used for the bulk transfer of offshore wind generation and cross-border electricity trades over long distances [1]. Their lifetime and reliability are strongly determined by the performance of insulation materials (e.g., cross-linked polyethylene, XLPE, and others) which will degrade under electrical over-stresses including space charge accumulation and the inception of electrical trees and partial discharges (PDs) caused by local defects [2]. Even though the severity of PD phenomena is reduced in DC cables compared to those operating at AC [3], the presence of ripples or transients in HVDC waveforms due to voltage modulation or transient events [4] can cause a rate-of-change in the electrical stress, increasing the risk and severity of PD [3].

Most research related to PD behaviour under DC power quality events has been performed by monitoring PD metrics of test samples under artificially distorted DC voltage profiles. In [5] the output of a single-phase half-wave rectifier was horizontally truncated at various levels and then applied to XLPE foils with air void defects, finding that the stress profile closer to a constant stress resulted in a higher PD inception voltage (PDIV) and a lower PD repetition rate. The stress waveforms simulating modular multilevel converter outputs were applied across a twisted pair test sample in [6], showing that a higher modulation level together with a lower switching frequency raised the PDIV and reduced the severity of PD, and vice-versa. Based on the theoretical harmonic content existing in the DC output of a 6-pulse voltage source converter, the voltage ripples with varying magnitudes were superimposed on a constant stress and applied across void-type epoxy resin disc samples in [7], where the time intervals between neighboring PD events were mostly in line with the period of the dominant harmonic; furthermore, intense PDs were more likely to occur around the greater ripple peaks.

However, existing literature lacks an appreciation of the fundamental evaluations of DC and increasing harmonic content and their impacts on PD pattern. The contributions of this paper are to investigate PD patterns in a needle-plane electrode configuration subject to DC stresses superimposed with various harmonic components that may exist in HVDC links. The PD behavior under pure AC or DC stress is first examined to ensure the functionality of the designed test circuit and identify the AC or DC PDIV separately. Then, Phase Resolved PD (PRPD) together with repetition rates and severity factors are evaluated for the PD measured under DC PDIV and (1.5 times) DC PDIV and its superimposing with a harmonic, respectively, offering insights into the potential effects of PD practical harmonics existing in insulation.

II. EXPERIMENTAL SETUP

A. Arrangements of Electrodes (Test Cell)

Fig. 1 provides a visual representation of the needle-plane electrode arrangement. The needle electrode, composed of carbon-steel, has a length of 25.6 mm and a tip with a 0.2 mm radius. The plane electrode, made of stainless steel, measures 50 mm in diameter and 7 mm in thickness. Both electrodes are vertically oriented. An insulating layer of Perspex, characterized by a relative dielectric constant of 3.6, is strategically placed on the plane electrode surface. The gap between the two electrodes is adjusted to 2 mm. This precisely arranged experimental setup serves as the foundation for the PD measurement investigation.

XXX-X-XXXX-XXXX-X/XX/$XX.00 ©20XX IEEE

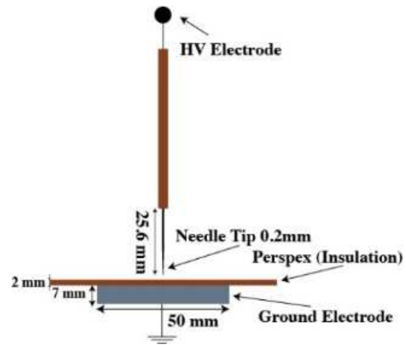

Fig. 1. Needle-plane test cell schematic

B. *Integration of DC and Harmonics*

Fig. 2 shows the experimental setup for measuring PD that involves the simultaneous use of AC and DC sources. A primary DC amplifier, which is rated at 50 kV with a current limit of 40 mA, is utilized alongside an amplifier capable of delivering a 10 kV output with a 10 mA current limit for the AC supply. The outputs of the AC and the DC amplifier are remotely and independently regulated by function generators. The output from the DC source, facilitated by a 100 MΩ current-limiting resistor, undergoes integration with the amplified AC voltage. This integration takes place through a low-pass filter circuit which is composed of a PD blocking resistor (1 MΩ) and a DC isolating capacitor (3.4 nF) arranged in series. Functioning as both a low-pass filter and an integration circuit, this setup allows low-frequency harmonics to pass through while effectively filtering out high-frequency noises.

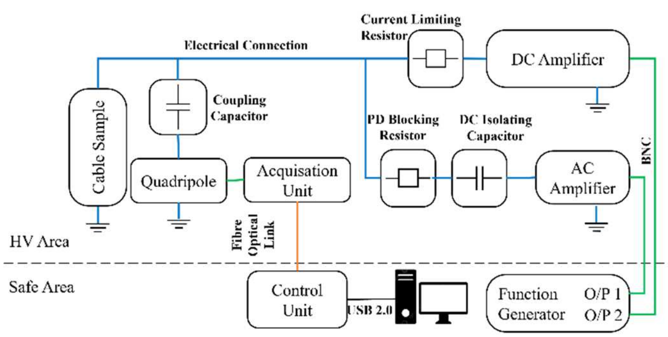

Fig. 2. Block diagram of the experimental setup

The test cell is aligned in parallel with a coupling capacitor and a PD measuring device. The resultant signal is channelled through the coupling capacitor (1 nF) before reaching the measuring device for a measurement of PD characteristics. The output from the measuring circuit is then routed to an acquisition system [8], which effectively segregates voltage and PD signals, ensuring precise measurements. Subsequently, these segregated signals are transmitted to a computer for the purpose of data acquisition and analysis. This integrated setup facilitates the measurement of PD in the needle-plane test cell.

The HV section of the setup is enclosed within a dedicated HV screened cage. A distinct secure space is allocated for the oversight of HV power supplies. This space functions as a central control hub for overseeing parameters such as the voltage across the test cell, PD signals, and the initiation of electrical discharges. To establish connections between the HV zone and the low-voltage control and monitoring region, a BNC interface and a fibre optical link are employed.

C. *Test Procedure*

The PD measurement setup, following IEC-60270 guidelines [9], was verified for absence of PD activity. Calibration with a 100 pC charge revealed environmental noises of 1.05 pC, surging to 3.86 pC with the interlock system. To ensure that any detected discharges genuinely originated from the test cell and were not merely noises, a 15 pC threshold was established for PD measurements.

With the setup calibrated, the initial testing phase involved the application of AC excitation to confirm that PD patterns were correctly generated and to establish a baseline for PDIV. DC stresses at different levels were applied across the test cell respectively to identify the PDIV which was defined as at least 10 PD discharges over a 10-minute interval under DC. Finally, PD pulses were continuously monitored for two hours where the PDIV or 1.5 times the PDIV was applied in the 1st hour and then superimposed with a particular harmonic component in the 2nd hour. The harmonic component was 10% of the DC voltage in magnitude and had a frequency ranging from 50 Hz to 1500 Hz, allowing for a comparison in the PD behaviour between the superimposing of harmonics at different frequencies. When PD measurements were completed a waiting period of at least 30 minutes was undertaken to depolarise the test circuit before starting the next test.

III. Results and Discussion

A. *Test under AC stress only*

To ensure the functionality of the designed test circuit, an AC voltage was applied to the needle-plane test configuration while maintaining zero DC input. The AC voltage was gradually increased to observe the occurrence of discharges which initiated at 3.7 kV rms, marking the PDIV point. A total of 2182 pulses were recorded over a 15-minute interval, which exhibited a well-known PRPD corona discharge pattern [10], as shown in Fig. 3(a).

To understand the discharge intensity and pattern at higher voltage levels, data recording sessions lasting 15 minutes each were conducted by incrementally increasing the AC voltage up to 5 kV rms. The resulting PRPD under 5 kV rms is shown in Fig. 3(b), indicating arrangement validation consistency with previously published work [10].

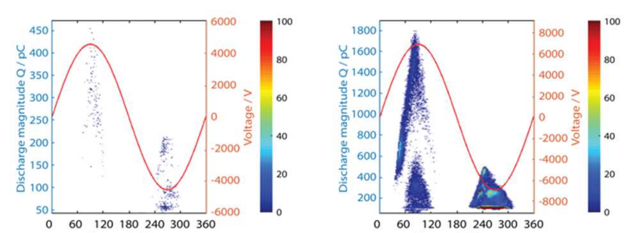

(a) Input at 3.7 kV rms in AC

(b) Input at 5 kV rms in AC

Fig. 3. Needle-plane corona discharge patterns under (a) the PDIV of 3.7 kV rms in AC and (b) 5 kV rms in AC. (The discharge intensity is presented by colormaps).

B. Test under DC stress only

It is noted that the methodology for determining the PDIV in DC differs from that in AC due to the presence of space charge accumulation phenomena. Various criteria have been adopted to ascertain PDIV in DC such as voltage causing 1 discharge per minute [11] or 5 discharges per minute [12]. In the absence of a standardised criterion, the minimum number of pulses required to define PDIV depends on the specific test object. In this work, the PDIV was established when 1 discharge per minute was met in a 10-minute interval, meaning that at least 10 pulses were recorded in the interval. Each voltage step was kept for 10 minutes, and this observation continued for 1 hour after reaching PDIV (i.e. about 2.5 kV in this work) to study the PD behaviour. Fig. 4 shows an example of the PD pulses over time under DC voltage.

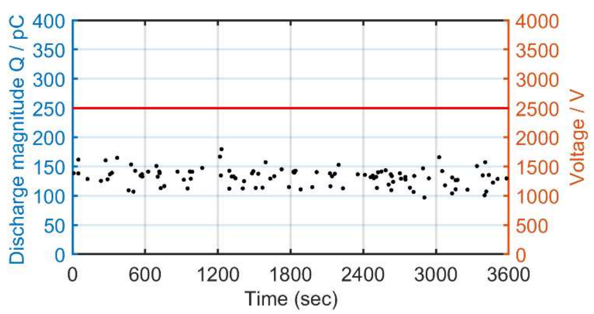

Fig. 4. Needle-plane discharge pattern under DC at the PDIV

C. Test under DC Superimposed with Harmonics.

In the tests of DC superimposed with harmonics, after the DC PDIV was applied for 1 hour to facilitate the cumulation of space charge, a particular harmonic frequency with 10% of the DC voltage in magnitude was introduced and sustained for another hour. Each harmonic frequency test was conducted twice such as Test 1 and Test 2 to ensure result repeatability. The results presented in Table I, indicate that higher harmonic frequencies lead to an increased number of discharge pulses. Notably, these pulses are predominantly concentrated in positive half-cycles, with minimal occurrences during negative half-cycles. This observation is attributed to the higher stress levels during positive half-cycles compared to negative half-cycles as depicted in Fig. 5.

TABLE I. PD PULSE NUMBERS IN THE TESTS OF PDIV WITH HARMONICS AT DIFFERENT FREQUENCIES

Harmonic Frequency	Number of Pulses					
	Test 1			Test 2		
	Total	+Ve	-Ve	Total	+Ve	-Ve
50 Hz	299	297	2	320	320	0
100 Hz	365	364	1	357	356	1
300 Hz	219	216	3	390	389	1
600 Hz	418	413	5	213	208	5
900 Hz	396	394	2	373	373	0
1200 Hz	510	506	4	474	473	1
1500 Hz	1214	1212	2	471	471	0

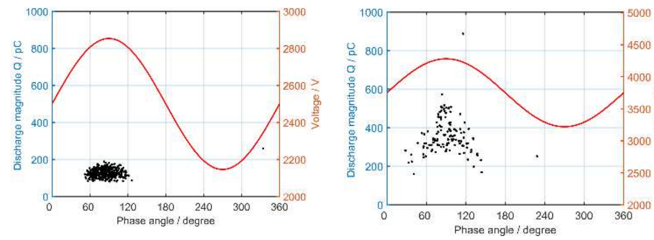

(a) PDIV plus 900 Hz Harmonics (b) 1.5*PDIV plus 900 Hz Harmonics

Fig. 5. The needle-plane discharge pattern under (a) the PDIV or (b) 1.5 times the PDIV in DC superimposed with 900 Hz harmonics.

To assess the influence of voltage amplitudes, the tests of DC superimposed with harmonics were repeated at a DC voltage level of 1.5 times PDIV. As an example, Fig. 5(b) shows the resulting PRPD pattern under 900 Hz harmonics, indicating that the voltage level growth results in an increase of the discharge magnitude. A quantitative comparison of the PD behaviour between the two voltage amplitudes is listed in Table II where the PD repetition rate is defined by the number of discharge pulses per second and the severity factor (SF) of PD is evaluated by (1) considering the dynamic or instantaneous variations in the occurrence time and magnitudes of PDs. The measurement of PD severity can potentially measure the insulation state of the test object [13].

$$SF = \frac{\sum_{n=1}^{N}(\frac{Q_n}{d_n})}{C} \tag{1}$$

where Q_n is the apparent charge (pC) of the n^{th} PD measured ($n = 1, \ldots, N$); C represents the number of sequential cycles of the harmonics during which PDs are measured (it is important to note that for the DC equivalent, the number of cycles considered is with respect to the harmonic frequency, as in DC there is no frequency); and the term d_n is defined by (2) based on the time intervals (seconds) between the n^{th} PD and its neighbouring PDs, denoted by Δt_{n-1} and Δt_n respectively.

$$d_n = \sqrt{{\Delta t_n}^2 + {\Delta t_{n-1}}^2} \tag{2}$$

Table II shows that repetition rates generally increase with the harmonic frequency and also with the voltage amplitude. However, the SF for 1.5 PDIV gives a very large value. These anomalies are attributed to the potential stray discharge pulses occurring in the DC PD test, which are unrelated to PD activity associated with any specific defect but possibly originate from space charge or external factors [14]. The absence of an equivalent C value for pure DC is the reason for the empty entry at 0 Hz in the SF table. Additionally, the superimposition of a 10% harmonic in the case of 1.5 PDIV with a frequency of 1500 Hz is not feasible due to limitations in the AC amplifier.

Moreover, Fig. 6 compares the SF of the PD recorded in the 1st hour under the pure DC PDIV against the SF estimated for the subsequent hour when a particular harmonic frequency was applied. The SFs are mostly shown to increase with the superimposing of harmonics, especially for those at higher frequencies. This implies that the existence of harmonics in HVDC voltage might exacerbate the PD occurring on insulation, potentially accelerating insulation degradation. However, it is important to note that the considered SF decreases in the case of pure DC, indicating that the formula is incorrectly used for DC due to the equivalent C value which is not really possible to translate directly to DC. A re-definition of the SF for pure DC is therefore required.

TABLE II. PD REPETITION RATES AND SEVERITY FACTORS IN TESTS OF PDIV OR 1.5*PDIV WITH HARMONICS AT DIFFERENT FREQUENCIES

Harmonic Frequency	Repetition Rate (pulse/sec)		Severity Factor (pC/sec)	
	PDIV	1.5*PDIV	PDIV	1.5*PDIV
0 Hz	0.0259	0.1395	-	-
50 Hz	0.0838	0.3114	0.0117	74.8724
100 Hz	0.1001	0.1537	0.0081	4.6002
300 Hz	0.0844	0.1705	0.0022	0.1257
600 Hz	0.0873	0.0473	0.2373	0.0006
900 Hz	0.1067	0.0378	0.0335	4.2789
1200 Hz	0.1364	2.2208	0.0589	5.6581
1500 Hz	0.2338	-	0.1560	-

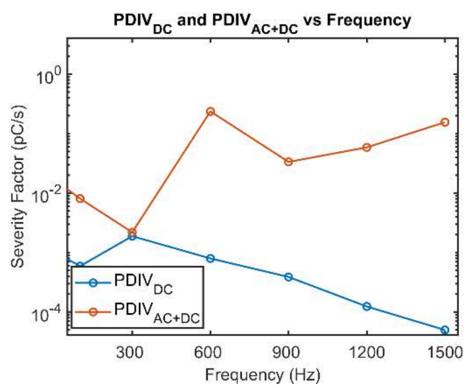

Fig. 6. SFs (pC/sec) of PDs in the 1st hour under the pure DC PDIV and in the subsequent hour with the superimposing of harmonics at different frequencies.

IV. CONCLUSIONS AND FUTURE WORK

PD occurring on defective HVDC insulation can degrade the insulation performance. To provide insights into the potential influences of harmonics existing in HVDC insulation scenarios on PD patterns, this paper has presented measurements of PD in a needle-plane electrode configuration with an insulation boundary subject to the superimposing of DC stresses with different harmonic frequencies. The PD has been found to mostly occur over the positive half-cycles of the voltage tested, where the electrical stress increases over the standard DC value; the negative half cycles have less stress and therefore it may be expected that PD will to some degree extinguish. The repetition rate appears to increase with voltage amplitude and increasing harmonic frequencies. In addition, the existence of harmonics on the DC voltage increases the severity of PDs.

Building on the test circuit designed, future experiments will replace the needle-plane electrode by cross-linked polyethylene insulation to measure PD patterns under a number of different practical arrangements. The influences of harmonics and transients observed in practical HVDC voltage data as well as cable sample temperatures on the PD behavior will also be examined.

ACKNOWLEDGMENT

The research was developed under the UK Engineering and Physical Sciences Research Council grant EP-T001445-1, and also a University of Strathclyde PhD Scholarship.

REFERENCES

[1] A. Stan, S. Costinas, and G. Ion, “Overview and assessment of HVDC current applications and future trends,” *Energies*, vol. 15, no. 3, p. 1193, Feb. 2022.

[2] G.C. Montanari, P. Morshuis, P. Seri, et al., “Ageing and reliability of electrical insulation: the risk of hybrid AC/DC grids,” *High Voltage*, vol. 5, no. 5, pp. 620-627, Oct. 2020.

[3] P.H.F. Morshuis and J.J. Smit, “Partial discharges at DC voltage: their mechanism, detection and analysis,” *IEEE Trans. Dielectr. Electr. Insul.*, vol. 12, no. 2, pp. 328-340, Apr. 2005.

[4] P.S. Wright, A. Bergman, A.-P. Elg, et al., “Onsite measurements for power-quality estimation at the Sweden-Poland HVDC link,” *IEEE Trans. Power Del.*, vol. 29, no. 1, pp. 472-479, Feb. 2014.

[5] P. Romano, G. Rizzo, C. Consolazione, et al., “The partial discharge behavior of different materials under DC periodic stress,” in *Proc. 2019 IEEE Conf. Electr. Insul. Dielectr. Phenomena (CEIDP)*, Washington, USA, pp. 661-665.

[6] P. Romano, A. Parastar, A. Imburgia, et al., “Partial discharge measurements under DC voltages containing harmonics produced by power electronic devices,” in *Proc. 2018 IEEE CEIDP*, Cancun, Mexico, pp. 558-561.

[7] E. Corr, A. Reid, X. Hu, et al., “Partial discharge testing of defects in dielectric insulation under DC and voltage ripple contents,” *CIGRE Science Eng.*, vol. 11, pp. 117-125, Jun. 2018.

[8] MPD 600 User Manual Version: MPD600.AE.7. OMICRON Electronics GmbH, Klaus, Austria.

[9] IEC60270, High Voltage Test Techniques - Partial Discharge Measurements. British Standards Institution, 1st ed., 2000.

[10] Florkowski, Marek, Dariusz Krześniak, Maciej Kuniewski, and Paweł Zydroń. 2020. "Partial Discharge Imaging Correlated with Phase-Resolved Patterns in Non-Uniform Electric Fields with Various Dielectric Barrier Materials" Energies 13, no. 11: 2676. https://doi.org/10.3390/en13112676

[11] A. Cavallini, G. Montanari, M. Tozzi, and X. Chen, “Diagnostic of HVDC systems using partial discharges,” *IEEE Trans. Dielectr. Electr. Insul.* vol. 18, no. 1, pp. 275-284, Feb. 2011.

[12] X. Feng, Q. Xiong, A.L. Gattozzi and R.E. Hebner, "Partial Discharge Experimental Study for Medium Voltage DC Cables," *IEEE Trans. Power Del.*, vol. 36, no. 2, pp. 1128-1136, Apr. 2021.

[13] B.G. Stewart, L. Yang, M. Judd, et al., “A simple metric for assessing the severity of partial discharge activity based on time-sequence-analysis-discharge level patterns,” *Trans. Electr. Electron. Mat.*. vol. 7, no. 6, pp. 313-318, Dec. 2006.

[14] S.A. Madhar, P. Mraz, A.R. Mor, and R. Ross, “Empirical analysis of partial discharge data and innovative visualization tools for defect identification under DC stress,” *Int. J. Electr. Power Energy Syst.*, vol. 123, p. 106270, Dec. 2020.